Preparation and Characterization of Sulfonated Syndiotactic Polystyrene Ionomers/Organoclay Nanocomposites

P. Govindaiah, S. R. Mallikarjuna, and C. Ramesh*

Division of Polymer Science & Engineering, National Chemical Laboratory, Pune 411008, India

Received June 30, 2006
Revised Manuscript Received September 2, 2006

Introduction. In recent years polymer/layered silicate nanocomposites have attracted great interest in both academia and industry because they often exhibit remarkable enhancement in material properties when compared with virgin polymers at very low filler loadings.[1−3] The enhancements in the properties of these materials are due to the interactions of the polymer chains with the surface of the clay layers and were maximum when the clay layers are completely delaminated or exfoliated in the polymer matrix.

When the surface energy of the polymer is too low, the interaction between the polymer and clay surfaces becomes difficult even if the clay surface was made organophilic. Introducing polar groups on sPS backbone can enhance surface energy of the polymers. Syndiotactic polystyrene (sPS) is an engineering semicrystalline thermoplastic material showing high melting point (about 270 °C), heat and chemical resistance, rapid crystallization, and good mechanical properties.[4−7] Reports on the synthesis of sPS/clay nanocomposites are very few mainly because of the high melting and processing temperatures. Furthermore, the low surface energy, because of the absence of polar groups, restricts sPS's interactions with polar polymers[8] or with organoclay. The conventional quaternary ammonium modified clays decompose at the processing temperatures.[9−12] To solve this problem, Park et al.[13,14] have utilized stepwise mixing procedure by mixing the organoclay with functionalized amorphous styrenic polymer followed by blending with sPS. Thermally stable modifiers based on phoshonium and imidazolium cations have been reported in the literature.[15−17] Tseng et al.[18] have used thermally stable modifiers based on cetylpyridinium ion for the preparation of sPS nanocomposites.

Recently, to improve the surface energy of semicrystalline polymers in the preparation of nanocomposites, many researchers introduced ionic groups on to the polymer chains. Moore et al. have introduced sodium sulfonate groups on poly(ethylene terephthalate)[19] and poly(butylene terephthalate)[20] backbone to get exfoliated organoclay. Nanocomposites prepared from ionomers of polypropylene,[21] polyethylene,[22,23] and a variety of other nonpolar thermoplastic polymers[24−26] also reveal good levels of organoclay exfoliation.

In this paper we describe the preparation and characterization of nanocomposites of sulfonated syndiotactic polystyrene (SsPS) ionomers with organoclay. For the first time we examined the effect of sulfonation content (sulfonation level ranging from 0.5 to 3.8 mol %) and type of ionomer (H^+, Na^+, K^+, and Rb^+ in the group I series of the periodic table) on intercalation/exfoliation of SsPS ionomers/organoclay nanocomposites by using wide angle X-ray diffraction (WAXD) and transmission electron microscopy (TEM). We have also studied the effect of clay layers on the crystallization of ionomers.

* Corresponding author. E-mail: c.ramesh@ncl.res.in.

Experimental Section. a. Materials. Syndiotactic polystyrene was kindly supplied by the Dow Chemical Co. The weight-average molecular weight was 275 000, and the melt index was 4.3. 1,1,2-Trichloroethane (TCE) and rubidium hydroxide were obtained from Aldrich. Potassium hydroxide, sodium hydroxide, and chloroform were purchased from Merck, India. The clay, Cloisite Na^+, was from Southern Clay Products. The reagents were of analytical reagent grade and were used as received. 1-Hexadecyl-2,3-dimethylimidazolium bromide was prepared in the laboratory by quaternizing 1,2-dimethylimidazole with hexadecyl bromide.

b. Preparation of Organoclay. Organoclay was prepared as per the standard exchange reaction.[27] The Na montmorillonite (10.0 g) with CEC 92 mequiv/100 g, *d* spacing 1.2 nm, was dispersed in water/methanol (60/40, v/v, 300 mL) by stirring with an overhead stirrer at room temperature for 2 h. 1-Hexadecyl-2,3-dimethylimidazolium bromide (4.4 g, 11.0 mmol) in a water/methanol mixture was poured into the dispersion of clay in drops and stirred for 24 h at 65 °C. Then the reaction mixture was cooled, centrifuged, and washed several times with distilled water and methanol until all the bromide ions were washed off, which was confirmed by testing the washings with $AgNO_3$. The organoclay obtained was freeze-dried under vacuum overnight. The organoclay was obtained as a fine dry powder. The organic content in the organoclay was determined from TGA analysis and found to be 25 wt %. The interlayer *d* spacing for the organo-modified montmorillonite was measured from WAXD and found to be 1.9 nm.

c. Preparation of SsPS Ionomers. SsPS was prepared as per the procedure reported elsewhere.[28−30] In a 1 L round-bottom flask syndiotactic polystyrene (6.5 g) and TCE/chloroform (60/40, v/v) mixture (500 mL) were stirred at reflux temperature (ca. 115 °C) until all the sPS was dissolved. Then the solution was cooled to 70 °C, and freshly prepared acetyl sulfate solution was added under vigorous stirring, which continued for 3 h. The amount of acetyl sulfate required was determined by the desired degree of sulfonation. Ethanol (10 mL) was added to arrest the reaction, and the polymer was precipitated by pouring the solution into diethyl ether (2 L) and filtered. It was washed with hot distilled water and then dried in a vacuum oven at 70 °C for 24 h. The polymer was redissolved in TCE and precipitated in excess of diethyl ether, filtered, and dried in a vacuum oven at 70 °C for 24 h. The degree of sulfonation was determined by nonaqueous titration.

The SsPS ionomers were prepared by fully neutralizing with addition of 20% excess methanolic alkali hydroxides (NaOH, KOH, and RbOH). The neutralized polymer solution was precipitated in diethyl ether, washed with hot methanol, and dried in a vacuum at 70 °C for 24 h.

d. Preparation of SsPS Ionomers/Clay Nanocomposites. SsPS ionomers/organoclay nanocomposites were prepared by the solution technique. Preweighed SsPS ionomers were dissolved in TCE at 120 °C, and then organoclay (8 wt %) was added and the solution kept at 90 °C for 10 h under constant agitation. The solvent was evaporated to obtain a translucent film. The sample was dried under vacuum at room temperature.

e. Characterization. The thermal properties of the samples were analyzed by a TA Instruments Q10 differential scanning calorimeter under standard conditions. The samples were heated under flowing nitrogen atmosphere from 0 to 300 °C at the rate of 10 °C/min and held for 1 min at the maximum temperature.

10.1021/ma061471u CCC: $33.50
Published on Web 09/19/2006

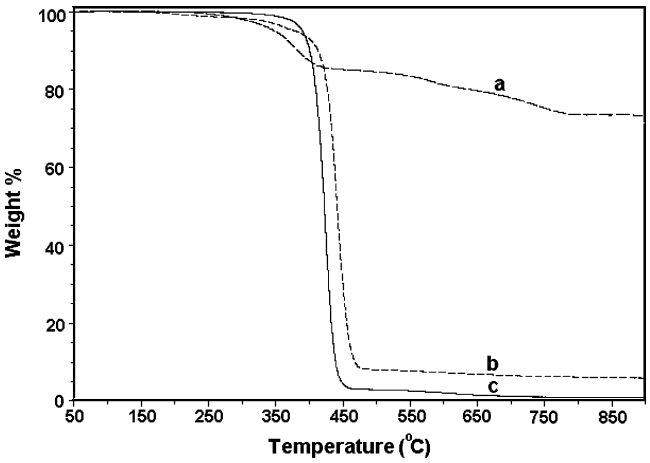

Figure 1. TGA thermogram of (a) organoclay, (b) RbSsPS 3.8 mol %/organoclay nanocomposite, and (c) RbSsPS 3.8 mol %.

At the end of holding period the sample was cooled at the rate of 10 °C/min to record the crystallization exotherm. The calorimeter was calibrated using standard protocols. The sample weight was about 5 mg in all the experiments. A TGA-7 unit in the Perkin-Elmer thermal analysis system was used to determine the thermal stability of the samples as well as the amount of clay present in the nanocomposites. The samples were heated under flowing nitrogen atmosphere from 50 to 900 °C at a heating rate of 10 °C/min, and the weight loss was recorded. The weight of the residue remaining at 900 °C was taken as the percent clay content in the nanocomposite and found to be 6 wt % for all the samples.

The WAXD experiments were performed using a Rigaku Dmax 2500 diffractometer equipped with a copper target and a diffracted beam monochromator. (Cu Kα radiation with $\lambda = 1.5406$ Å) with a 2θ scan range of $2-10°$ at room temperature. The specimen of nanocomposites for WAXD was thin film samples melt-pressed on a copper block sample holder at 280 °C for a period of 15 s. Samples for TEM were sectioned using a Lieca Ultracut UCT microtome with thicknesses of 50−60 nm using a diamond knife at room temperature. Before sectioning for TEM, the samples were heated to 280 °C for a period of 10−15 s and sized the sample so that it could be conveniently held on the sample holder of the microtome for sectioning. The sections were collected from water on 300 mesh carbon-coated copper grids. TEM imaging was done using a JEOL 1200EX electron microscope operating at an accelerating voltage of 80 kV. The density of clay particles is enough to produce contrast between polymer and clay stacks; hence, staining was not required. Images were captured using a charged couple detector (CCD) camera for further analysis using Gatan Digital Micrograph analysis software.

Results and Discussion. The organoclay used in the present study is obtained by modification of pristine Na^+ montmorillonite with 1-hexadecyl-2,3-dimethylimidazolium cation. Figure 1 shows the TGA thermograms of the organoclay (a), RbSsPS 3.8 mol %/organoclay nanocomposites (b), and RbSsPS 3.8 mol % (c). The organic content in the organoclay was found to be 25 wt % which is obtained as the weight loss at 900 °C, which matches with the calculated 100% cation exchange capacity. The onset of degradation of the modifier in the organoclay (295 °C, 2% weight loss) is higher than the melting temperature of sPS, which is around 270 °C. As expected from the improved stability of the modifier, the nanocomposite also exhibits thermal stability up to 300 °C, and the degradation sets in above 300 °C.

Figure 2a shows the WAXD pattern for the unmodified clay, modified clay, sPS, and the sPS/organoclay nanocomposite. The unmodified clay has a gallery height of 1.24 nm, and upon modification it increases to 1.90 nm. The sPS/clay nanocomposite shows two peaks due to clay at $2\theta = 4.20°$ and at 4.65°, and the *d* spacings are 2.10 and 1.90 nm, respectively. This indicates that in the nanocomposite the sPS penetrate into a fraction of the clay galleries, and the gallery expands to 2.10 nm. The presence of peak at 4.65° indicates that some amount of organoclay remains without intercalation. The peak at around $2\theta = 6.8°$ in the sPS and sPS/organoclay nanocomposite is due to the 110 reflection of the α crystalline form. The nanocomposites as prepared by the solution technique exhibit δ form, but on heating above 200 °C all the samples exhibit only the α form and such behavior is similar to the well-established behavior of sPS.[31] The polymorphism and the crystalline transition of SsPS will be the subject of another paper and will not be discussed in detail here. The TEM micrograph in Figure 2b shows agglomerated structures, which further implies that the organoclay tactoids remain intact and are consistent with WAXD data. This type of behavior exhibited by sPS/organoclay nanocomposites may be due to the limited interaction of sPS with the organoclay layers as the surface energy of the sPS is low. It has been shown that intercalation/exfoliation can be obtained with suitable organoclay.[18,32,33] However, with the present organoclay only the agglomerated structures are obtained, and this may be due to the choice of the modifier.[34]

Converting the sPS into sPS ionomers improves the interaction of the sPS with organoclay, and Figure 3 shows the X-ray diffraction pattern of SsPS ionomer/organoclay nanocomposites with various degree of sulfonation and different ion types (H^+, Na^+, K^+, and Rb^+). Table 1 shows the gallery height of the clays for various ionomer/organoclay nanocomposites. The WAXD patterns in Figure 3a show that as the extent of sulfonic acid groups in sPS increases from 0.5 to 3.8 mol %, the interlayer *d* spacing of the organoclay increases gradually from 1.9 to 2.9 nm, demonstrating that higher the sulfonation levels lead to better intercalation in the nanocomposites. Similarly, Figure 3b shows that for the sodium salt of SsPS ionomer (NaSsPS)/organoclay nanocomposites 0.5 mol % ionomer content shows little intercalation, while the extent of intercalation gradually increased up to 3.4 nm with the increase in the ionomer content to 3.8 mol %.

In Figure 3c,d SsPS/organoclay nanocomposites prepared with K^+ and Rb^+ ionomers show intercalation of polymer chains in to the organoclay gallery at lower levels of ionomeric content such as 0.5 mol %, while higher levels of ionomeric content show disappearance of the peaks due to clay, indicating completely delaminated and disordered structure for the organoclay in the nanocomposites. Overall, it can be clearly understood from the above trends that, irrespective of the ionomer cation type, the extent of dispersion of the organoclay in the polymer matrix has improved with the increase in ionomer content. This type of behavior is obvious from the fact that as the ionomer content increases, the surface energy of the polymer increases, which in turn increases the interaction of the polymer with the organoclay.

It is also of interest to see whether the increased surface energy of the polymer is sufficient to intercalate/exfoliate the unmodified clay. To that end nanocomposites of various ionomers with highest ionomer content of 3.8 mol % were prepared with unmodified clay, and the X-ray diffraction pattern is shown in Figure 4. In all the samples the clay peak shows no significant shift, indicating the absence of intercalation of the polymer into the gallery. These results indicate that the increased

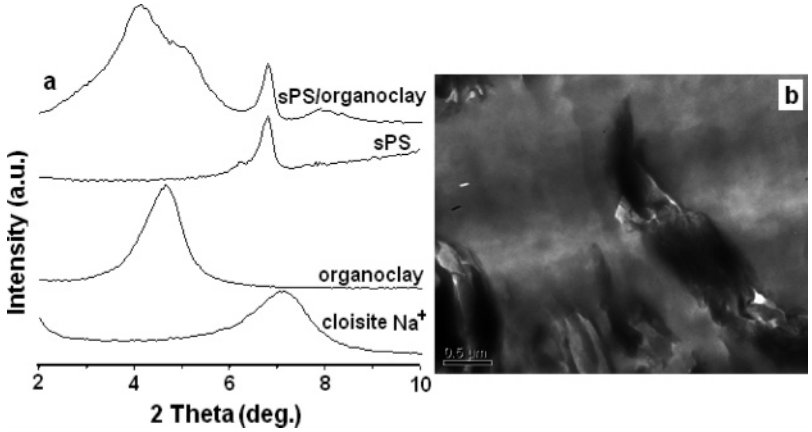

Figure 2. (a) WAXD pattern of cloisite Na^+, organoclay, sPS, and sPS/organoclay nanocomposite. (b) TEM micrograph of sPS/organoclay nanocomposite.

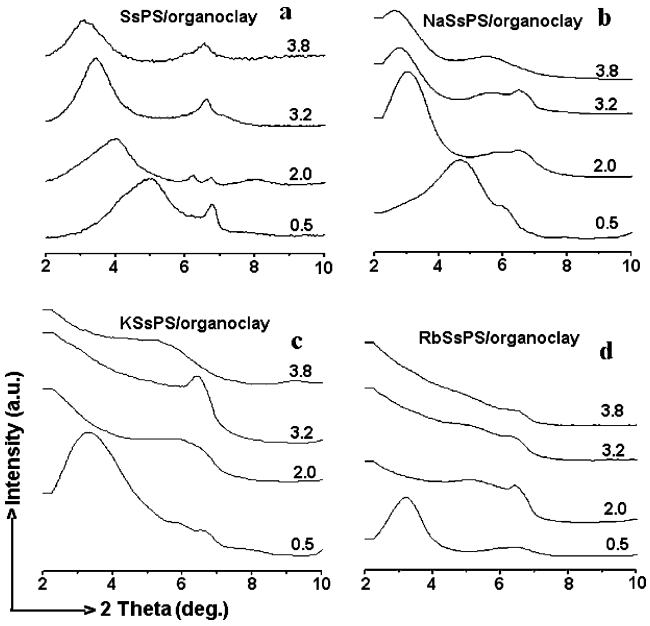

Figure 3. WAXD pattern of SsPS ionomer/organoclay nanocomposites with different ionomer content and cation type (a) H^+, (b) Na^+, (c) K^+, and (d) Rb^+.

Table 1. Clay Gallery Height from WAXD Data of SsPS Ionomers/ Clay Nanocomposites

	clay gallery height (nm)			
sulfonation level (mole %)	H^+	Na^+	K^+	Rb^+
0.5	1.84	1.90	2.63	2.72
2.0	2.20	2.94	*a*	*a*
3.2	2.60	3.15	*a*	*a*
3.8	2.90	3.40	*a*	*a*

[a] Exfoliated.

level of surface energy of the polymer achieved in the present work is not sufficient to interact with unmodified clay and necessitates the need for the clay modification for interacting with polymer. Furthermore, it shows that the nature of surface treatment will have a significant effect on the interaction between the clay and the polymer.[34]

It is interesting to note that the extent of interaction of the SsPS ionomer with organoclay depends on the type of cation in the SsPS ionomers. Even for low level of sulfonation, i.e., with 0.5 mol % ionomer content of SsPS, with the change of cations from H^+ to Rb^+ in the SsPS ionomer/organoclay nanocomposites, the WAXD patterns show systematic changes

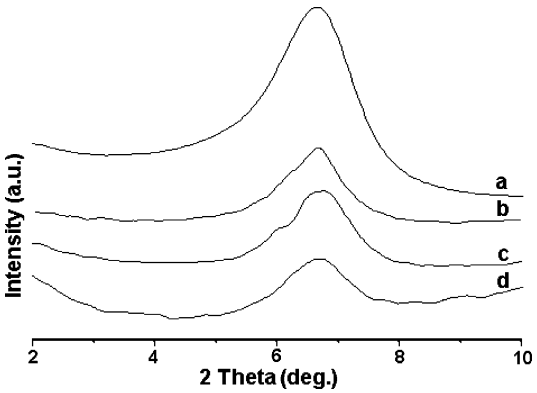

Figure 4. WAXD pattern of 3.8 mol % SsPS ionomers/cloisite Na^+ nanocomposites with different cations: (a) cloisite Na^+, (b) NaSsPS/ cloisite Na^+, (c) KSsPS/cloisite Na^+, and (d) RbSsPS/cloisite Na^+

in the gallery height. The gallery height increases marginally from 1.8 to 1.9 nm when the H^+ is changed to Na^+. However, when the cation is changed to K^+ and Rb^+, the gallery height increases to 2.6 and 2.7 nm, respectively, indicating a high level of intercalation. Similarly, when the ionomer content was higher (2−3.8 mol %), for H^+ and Na^+ cations in the SsPS ionomer/ organoclay nanocomposites, the WAXD pattern shows increase in the organoclay *d* spacing, indicating that the polymer chains have penetrated into the organoclay interlayer gallery. On the other hand, for K^+ and Rb^+ cations in the SsPS ionomer/ organoclay nanocomposites, the WAXD patterns show the disappearance of the peak due to the organoclay, indicating exfoliation of organoclay in the polymer matrix. Here also it can be noted that the extent of intercalation increased with the change in the cation type from H^+ to Na^+ and lead to exfoliations in the case of K^+ and Rb^+. The structure of the nanocomposites with various cations was further confirmed by TEM analysis. The typical TEM micrographs of SsPS ionomer/ organoclay nanocomposites with an ionomer content of 3.8 mol % with various cations are shown in Figure 5. The parallel lines observed in the micrograph in Figure 5a,b indicate that intercalated nanocomposites were obtained with H^+ and Na^+ SsPS/organoclay nanocomposites, and the distance between the parallel lines measured from the micrographs is comparable with the *d* spacing obtained from WAXD. Figure 5c,d shows the TEM micrograph of SsPS ionomers/organoclay nanocomposite with K^+ and Rb^+ cations, revealing that the clay layers are completely delaminated and exfoliated in the polymer matrix.

The extent of intercalation/exfoliation of the polymer with the organoclay depends on the extent of interaction of the

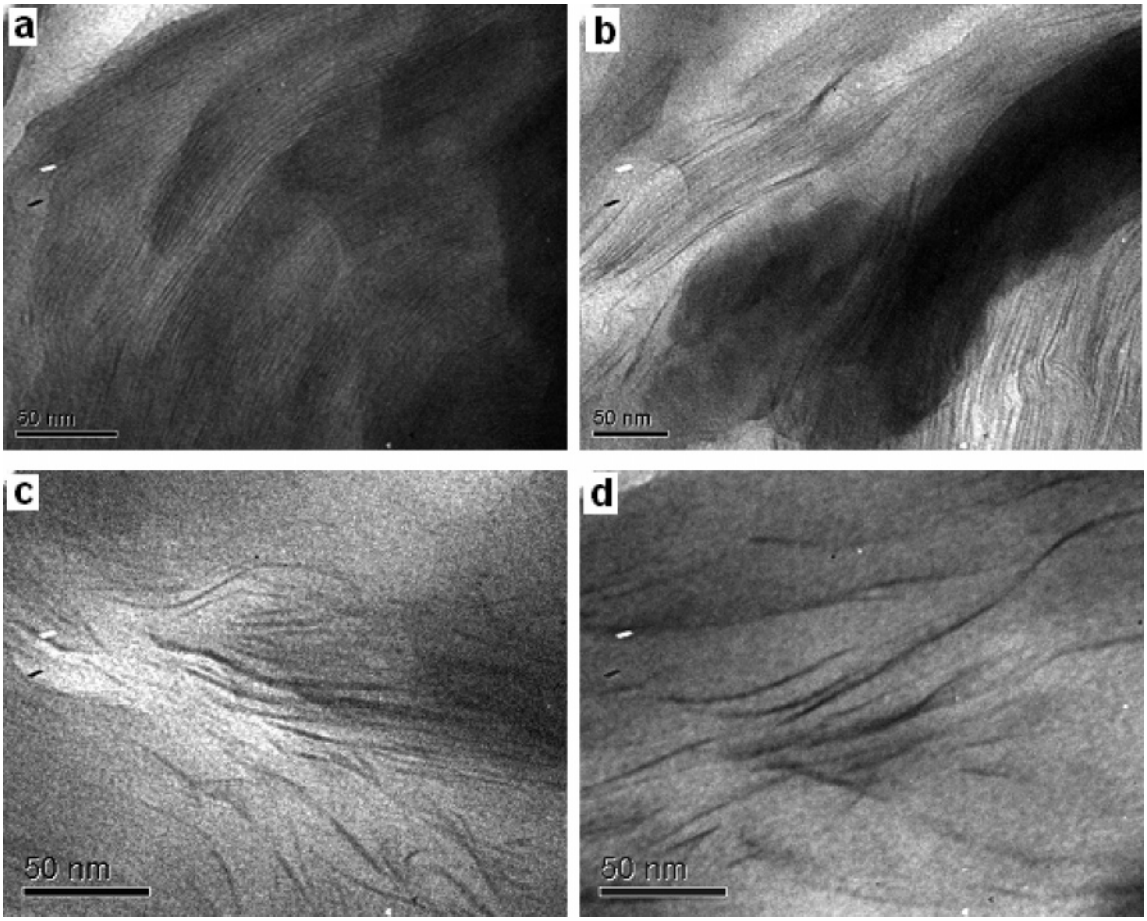

Figure 5. TEM micrographs of SsPS ionomers 3.8 mol %/organoclay nanocomposites (a) SsPS, (b) NaSsPS, (c) KSsPS, and (d) RbSsPS.

polymer with the organoclay surface. The higher the polarity of the polymer, the better the interaction with the organoclay, which has a higher polarity and surface energy. In the above results it was observed that as the cation of the SsPS ionomer in the nanocomposites changed from H^+ to Rb^+, the interlayer distance (*d* spacing) increase and even leads to exfoliation in the case of K^+ and Rb^+ cation. This behavior of better interaction with change in cations from H^+ to Rb^+ may be attributed to the increase in polarity of the ionomeric salt. It is known that as we move down the group in the periodic table, with the increase in the size of the cation, the polarizability of the cation increases as indicated by absolute hardness parameters for the cations.[35] As the polarizability of the cations in SsPS ionomers increases from H^+ to Rb^+, the interaction with the organoclay increases and resulted in exfoliation.

The interaction of the polymer with clay layers has a profound influence on the melt crystallization of the sPS ionomer. The crystallization peak temperature (T_{CC}) on cooling from melt has been taken as a measure of crystallization rate.[36] High T_{CC} during cooling in nonisothermal experiments indicates higher crystallization rate. Table 2 gives the T_{CC} on cooling from the melt for various samples. The T_{CC} decreases with increasing sulfonation level, indicating inhibition in crystallization. The crystallization is further inhibited when the H^+ ion is replaced by different cations like Na^+, K^+, and Rb^+. At higher sulfonation levels, ca. 3.8% most of the samples do not crystallize on cooling from the melt. The NaSsPS samples are the most affected, while RbSsPS samples showed relatively better crystallization rate under comparable cooling rate. The reduction in the crystallization rate of these samples is attributed to the ionic aggregation arising due to the Coulombic interactions between the ion pairs which impedes the chain mobility.[37] The Coulombic interactions between the ion pair become weaker with increasing size of the alkali ions.[38,39] The RbSsPS samples have lesser Coulombic interactions and fewer aggregations of ions compared to NaSsPS samples. Hence, RbSsPS samples have a better crystallization rate compared to NaSsPS, while the KSsPS samples takes the middle position.

Table 2. Crystallization Temperature on Cooling from the Melt for Various Samples

	crystallization temperature (°C)							
	without clay				nanocomposite			
sulfonation level (mole %)	H^+	Na^+	K^+	Rb^+	H^+	Na^+	K^+	Rb^+
0.5	234	233	233	232	234	236	236	236
2.0	225	199	189	193	228	209	218	223
3.2	222	183	183	194	222	205	215	222
3.8	212	*a*	*a*	*a*	212	163	184	198

[a] Do not crystallize on cooling from the melt.

The clay layers apparently do not influence the crystallization of the sulfonated samples as evident from the crystallization temperatures of the SsPS nanocomposites shown in Table 2. On the other hand, clay layers enhance the crystallization rate of the samples having alkali metal ions. As an example, it is clearly seen in the case of the sample sulfonated to 3.8% and neutralized with K^+ does not crystallize on cooling and remains amorphous. But in the nanocomposite it crystallizes at 184 °C, indicating that the crystallization rate has improved. In the case of samples sulfonated to lower levels, the crystallization peaks appear at higher temperatures than the samples without clay, indicating faster crystallization rates in the case of nanocomposites. These indicate that the clay layers modified with

1-hexadecyl-2,3-dimethylimidazolium cation prevents the aggregation of ions, and the crystallization rate increases. It is clear from Table 2 that the exfoliated nanocomposites showed better crystallization rate than the intercalated ones because of the uniformly dispersed clay layers in the polymer matrix.

Conclusion. The interaction of sPS with organoclay was improved by increasing the surface energy of the polymer by introducing the polar ionic functional groups such as ionomers of sulfonic acids with H^+, Na^+, K^+, and Rb^+ cations. It was demonstrated that higher ionomer content leads to better interaction with the polar silicate surface of the organoclay, resulting in better intercalation/exfoliation. For the first time we have shown that increasing the size and polarizability of the cation from H^+ to Rb^+ resulted in improved intercalation/exfoliation behavior even with low levels of ionomer content. The SsPS ionomers show lower crystallization rates compared to sPS due to ionic aggregation. However, in the case of SsPS ionomer nanocomposites, the interaction of the modified clay layers with the ionomer leads to less aggregation and partially restores the crystallization rates.

Acknowledgment. The authors thank Dr. S. Sivaram, Director, and National Chemical Laboratory for his keen interest and encouragement during the course of this work. Authors also thank Dr. C. V. Avadhani, PSE Division, for his help during the sulfonation of sPS and Mr. R. S. Gholap for his help during TEM measurements.

References and Notes

(1) LeBaron, P. C.; Wang, Z.; Pinnavaia, T. J. *Appl. Clay Sci.* **1999**, *15*, 11.
(2) Alexander, M.; Dubois, P. *Mater. Sci. Eng.* **2000**, *28*, 1.
(3) Ray, S. S.; Okamoto, M. *Prog. Polym. Sci.* **2003**, *28*, 1539.
(4) Woo, E. M.; Sun, Y. S.; Lee, M. L. *Polymer* **1999**, *40*, 4425.
(5) Vittoria, V.; Filho, A. R.; De Candia, F. *J. Macromol. Sci., Phys.* **1990**, *B29*, 411.
(6) Cimmino, S.; Pace, E. Di; Martuscelli, E.; Silvestre, C. *Polymer* **1991**, *32*, 1080.
(7) De Rosa, C.; Rapacciuolo, M.; Guerra, G.; Petraccone, V. *Polymer* **1992**, *33*, 1423.
(8) Molner, A.; Eisenberg, A. *Polym. Eng. Sci.* **1992**, *32*, 1665.
(9) Xie, W.; Gao, Z.; Pan, W.-P.; Vaia, R.; Hunter, D.; Singh, A. *Polym. Mater. Sci. Eng.* **2000**, *83*, 284.
(10) Xie, W.; Goa, Z.; Lui, K.; Pan, W. P.; Vaia, R.; Hunter, D.; Singh, A. *Thermochim. Acta* **2001**, *367*, 339.
(11) Jones, M., Jr. *Organic Chemistry*, 2nd ed.; W. W. Norton & Co.: New York, 2000; p 258.
(12) Wright, A. C.; Granquist, W. T.; Kennedy, J. V. *J. Catal.* **1972**, *25*, 65.
(13) Park, C. I.; Park, O. O.; Lim, J. G.; Kim, H. J. *Polymer* **2001**, *42*, 7465.
(14) Park, C. I.; Choi, W. M.; Kim, M. H.; Park, O. O. *J. Polym. Sci., Polym. Phys.* **2004**, *42*, 1685.
(15) Zhu, J.; Morgan, A. B.; Lamelas, F. J.; Walkie, C. A. *Chem. Mater.* **2001**, *13*, 3774.
(16) Gilman, J. W.; Awad, W. H.; Davis, R. D.; Shields, J.; Harris Jr., R. H.; Davis, C.; Morgan, A. B.; Sutto, T. E.; Callahan, J.; Trulove, P. C.; DeLong, H. C. *Chem. Mater.* **2002**, *14*, 3776.
(17) Xie, W.; Xie, R.; Pan, W.; Hunter, D.; Koene, B.; Tan, L.; Vaia, R. *Chem. Mater.* **2002**,*14*, 4837.
(18) Tseng, C. R.; Wu, J. Y.; Lee, H. Y.; Chang, F. C. *Polymer* **2001**, *42*, 10063.
(19) Barber, G. D.; Calhoun, B. H.; Moore, R. B. *Polymer* **2005**, *46*, 6706.
(20) Chisholm, B. J.; Moore, R. B.; Barber, G.; Khouri, F.; Hempstead, A.; Larsen, M.; Olson, E.; Kelley, J.; Balch, G.; Caraher, J. *Macromolecules* **2002**, *35*, 5508.
(21) Wang, Z. M.; Nakajima, H.; Manias, E.; Chung, T. C. *Macromolecules* **2003**, *36*, 8919.
(22) Shah, R. K.; Paul, D. R. *Macromolecules* **2006**, *39*, 3327.
(23) Lee, J. A.; Kontopoulou, M.; Parent, J. S. *Polymer* **2005**, *46*, 5040.
(24) Start, P. R.; Mauritz, K. A. *J. Polym. Sci., Polym. Phys.* **2003**, *41*, 1563.
(25) Kovarova, L.; Kalendova, A.; Malac, J.; Vaculik, J.; Malac, Z.; Simonic, J. *Annu. Tech. Conf. Soc. Plast. Eng.* **2002**, *60*, 2291.
(26) Barber, G. D.; Carter, C. M.; Moore, R. B. *Annu. Technol. Conf. Soc. Plast. Eng.* **2000**, *58*, 3763.
(27) Vaia, R. A.; Teukolsky, R. K.; Giannelis, E. P. *Chem. Mater.* **1994**, *6*, 1017.
(28) Govindaiah, P.; Avadhani, C. V.; Ramesh, C. *Macromol. Symp.* **2006**, *241*, 88.
(29) Orler, E. B.; Yontz, D. J.; Moore, R. B. *Macromolecules* **1993**, *26*, 5157.
(30) Li, H. M.; Liu, J. C.; Zhu, F. M.; Lin, S. A. *Polym. Int.* **2001**, *50*, 421.
(31) Gowd, E. B.; Nair, S. S.; Ramesh, C. *Macromolecules* **2002**, *35*, 8509.
(32) Ghosh, A. R.; Woo, E. M. *Polymer* **2004**, *45*, 4749.
(33) Tseng, C. R.; Lee, H. Y.; Chang, F. C. *J. Polym. Sci., Part B* **2001**, *39*, 2097.
(34) Shah, R. K.; Hunter, D. L.; Paul, D. R. *Polymer* **2005**, *46*, 2646.
(35) Pearson, R. G. *Inorg. Chem.* **1988**, *27*, 734.
(36) Pilati, F.; Toselli, M.; Messori, M.; Manzoni, C.; Turturro, A.; Gattiglia, E. G. *Polymer* **1997**, *38*, 4469.
(37) Orler, E. B.; Moore, R. B. *Macromolecules* **1994**, *27*, 4774.
(38) Lu, X.; Steckle, W. P.; Weiss, R. A. *Macromolecules* **1993**, *26*, 5876.
(39) Hird, B.; Eisenberg, A. *Macromolecules* **1992**, *25*, 6466.

MA061471U